# AUGMENTED LAGRANGIAN FORMULATION AND SENSITIVITY ANALYSIS OF CONTACT PROBLEMS

## Stanisław Stupkiewicz

Institute of Fundamental Technological Research
Polish Academy of Sciences
Świętokrzyska 21, 00–049 Warsaw, Poland
e-mail: sstupkie@ippt.gov.pl, web page: http://www.ippt.gov.pl

**Key words:** Frictional contact, Augmented Lagrangian formulation, Sensitivity analysis, Direct Differentiation Method.

**Abstract.** *In this paper the sensitivity analysis is developed for frictional contact problems in augmented Lagrangian formulation. Importantly, unlike in previous developments, the exact sensitivity analysis results in a non-iterative sensitivity problem to be solved at each time increment of a path-dependent direct problem. The finite element implementation is performed within the* Computational Templates *environment. Examples of sensitivity analysis and optimisation of two-dimensional frictional contact problems illustrate the approach.*

1

# 1  INTRODUCTION

Several developments of sensitivity analysis for frictional contact problems have recently been reported employing the penalty formulation of contact and friction conditions [1, 2], or the augmented Lagrangian formulation [3]. Generally, the sensitivity analysis framework for path-dependent problems, such as those in elasto-plasticity [4, 5, 6], can directly be applied also for frictional contact problems. However, the common approach to the augmented Lagrangian method, which employs the Uzawa algorithm, implies that the exact sensitivity analysis is not a single linear problem, but requires iterations corresponding to the iterative update scheme for Lagrange multipliers. This is avoided in [3] by solving an approximate non-iterative sensitivity problem in which oversized penalties are used. A more detailed discussion of the consequences of the Uzawa algorithm on the sensitivity analysis is provided in Section 3.3.

In this work, an alternative approach [7, 8] to the augmented Lagrangian treatment of contact and friction inequality constraints is adopted, which leads to the full Newton solution of the saddle-point problem in primal and dual variables. This formulation is particularly suitable for sensitivity analysis, as the direct differentiation method leads to a non-iterative linear sensitivity problem at each load increment. Moreover, the operator of the sensitivity problem is exactly the tangent operator of the iterative Newton scheme of the direct problem.

The paper is organized as follows. The general sensitivity analysis framework for path-dependent problems is provided in Section 2. In Section 3 the formulation of a contact problem is provided and it is demonstrated that the finite element problem to be solved fits into the general framework of sensitivity analysis of Section 2. For brevity of exposition, only the frictionless contact of an elastic body with a rigid obstacle is considered in detail in Section 3, but the extensions to general contact problems are also discussed. The finite element implementation is briefly described in Section 4. Numerical examples are provided in Section 5. The shape sensitivity analysis of selected two-dimensional problems is performed in order to verify the accuracy of the DDM-based sensitivity analysis. A simple, metal forming-oriented shape optimisation problem is also presented.

# 2  GENERAL FRAMEWORK OF SENSITIVITY ANALYSIS

The general framework of sensitivity analysis of path-dependent problems is briefly outlined in this section. The direct differentiation method (DDM) is applied for discretized problems. The exposition is based on the work of Michaleris et al. [6], where more details can be found, including the adjoint system approach.

Consider the residual form of a nonlinear path-dependent problem at time $t = t_{n+1}$ (e.g. resulting from a standard finite element spacial and temporal discretization)

$$\mathbf{R}(\mathbf{U}, {}^n\mathbf{U}) = \mathbf{0},\tag{1}$$

where $\mathbf{U}$ is the global response vector at $t = t_{n+1}$ and ${}^n\mathbf{U}$ is the response at $t = t_n$. Here the time at which the quantity is evaluated is denoted by a left superscript and for brevity

the superscript $n+1$ denoting the *current* value of the quantity (i.e. referring to the end of the considered time step) is omitted. The *previous* response ${}^n\mathbf{U}$ is known from the solution of the corresponding equation (1) at time $t = t_n$. Problem (1) is called a *direct* (or *primal*) problem.

The direct problem (1), constituting the set of nonlinear equations, is solved for the *current* response $\mathbf{U}$ using the iterative Newton scheme ($I$ being the iteration number), i.e. the following two steps are repeated until the convergence is obtained

$$\delta\mathbf{U}^I = -\left(\left.\frac{\partial\mathbf{R}}{\partial\mathbf{U}}\right|_{\mathbf{U}=\mathbf{U}^I}\right)^{-1}\mathbf{R}(\mathbf{U}^I, {}^n\mathbf{U}), \quad \mathbf{U}^{I+1} = \mathbf{U}^I + \delta\mathbf{U}^I. \tag{2}$$

The problem and thus also the response are assumed to depend on a design parameter $\phi$ representing any material or shape parameter. Rewrite the residual equation (1) so that the dependencies on $\phi$ are expressed explicitly

$$\mathbf{R}[\mathbf{U}(\phi), {}^n\mathbf{U}(\phi), \phi] = \mathbf{0}. \tag{3}$$

The solution of the direct problem depends on the design parameter in an implicit way through the problem equation as indicated in Eq. (3). The derivative of this implicit relation is called the *response sensitivity*.

Consider now a general response functional (representing for example an objective function or a constraint in a design optimisation or inverse problem)

$$F(\phi) = G[{}^1\mathbf{U}(\phi), \ldots, {}^M\mathbf{U}(\phi), \phi], \tag{4}$$

which can be defined in terms of response ${}^n\mathbf{U}$ at any time $t_n$, $n = 1, \ldots, M$. The sensitivity of $F$ is obtained by differentiating Eq. (4) with respect to $\phi$, namely

$$\frac{\mathrm{D}F}{\mathrm{D}\phi} = \frac{\partial G}{\partial {}^1\mathbf{U}}\frac{\mathrm{D}{}^1\mathbf{U}}{\mathrm{D}\phi} + \cdots + \frac{\partial G}{\partial {}^M\mathbf{U}}\frac{\mathrm{D}{}^M\mathbf{U}}{\mathrm{D}\phi} + \frac{\partial G}{\partial\phi}. \tag{5}$$

In order to distinguish the derivatives corresponding to the explicit and implicit dependencies the latter are denoted by $\mathrm{D}\cdot/\mathrm{D}\phi$, cf. Eq. (5). In the direct differentiation method, the unknown response sensitivities $\mathrm{D}\mathbf{U}/\mathrm{D}\phi$ are found by solving the *sensitivity problem*

$$\frac{\partial\mathbf{R}}{\partial\mathbf{U}}\frac{\mathrm{D}\mathbf{U}}{\mathrm{D}\phi} = -\left(\frac{\partial\mathbf{R}}{\partial {}^n\mathbf{U}}\frac{\mathrm{D}{}^n\mathbf{U}}{\mathrm{D}\phi} + \frac{\partial\mathbf{R}}{\partial\phi}\right), \tag{6}$$

which is obtained by taking the total derivative of Eq. (3) with respect to the design parameter $\phi$. The right-hand side of Eq. (6) is the *sensitivity pseudo-load vector*.

The sensitivity problem (6) can be solved for the current response sensitivity $\mathrm{D}\mathbf{U}/\mathrm{D}\phi$ once the previous response sensitivity $\mathrm{D}{}^n\mathbf{U}/\mathrm{D}\phi$ is known as a solution of the sensitivity problem at the previous time increment. The sensitivity problem is thus path-dependent.

It can effectively be solved simultaneously with the direct problem since it is linear and the operator in Eq. (6) is the tangent stiffness matrix of the direct problem (2).

The above scheme of sensitivity analysis has to be extended when problems involving state variables (e.g. elasto-plasticity, frictional contact) are considered. This is because in addition to the global equilibrium equations, the local constitutive problems have to be solved. The corresponding iteration-subiteration procedure is described in [6] (the case of *transient coupled nonlinear systems*). The discussion of topics related to non-differentiability, which is naturally expected in contact problems (but in elasto-plasticity as well) can be found in [2], see also [9].

## 3 ELASTIC FRICTIONLESS CONTACT PROBLEM

For clarity and brevity of presentation, only the frictionless contact of an elastic body with a rigid obstacle is considered in this section. Note, however, that generalizations for the case of inelastic problems, frictional interaction and multi-body contact can be found in numerous works, see for example recent books [10, 11] and references therein.

### 3.1 Contact problem as a constrained minimisation problem

Consider an elastic body represented by a domain $\Omega^0 \subset \mathcal{R}^3$ in its reference configuration. Displacements $\bar{\mathbf{u}}$ and (nominal) tractions $\bar{\mathbf{t}}$ are prescribed on parts $\Gamma_u^0$ and $\Gamma_t^0$, respectively, of the boundary of $\Omega^0$, and $\Gamma_c^0$ is a surface of potential contact of the body with a rigid obstacle. The respective parts of the boundary in the deformed configuration $\Omega$ are denoted by $\Gamma_u$, $\Gamma_t$ and $\Gamma_c$, cf. Fig. 1. The rigid obstacle is represented by a smooth surface $\Gamma_c'$.
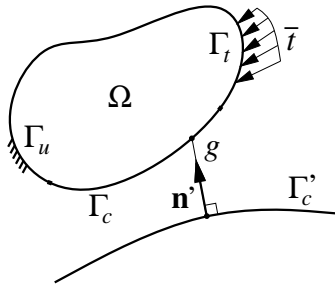


Figure 1: Frictionless contact with a rigid obstacle.

A gap function $g$ defining the distance of the body from the obstacle is defined for each point of the potential contact surface $\mathbf{x} \in \Gamma_c$ by

$$g = (\mathbf{x} - \mathbf{x}') \cdot \mathbf{n}', \tag{7}$$

where $\mathbf{x}' \in \Gamma_c'$ is an orthogonal projection of $\mathbf{x}$ on $\Gamma_c'$ and $\mathbf{n}'$ is a unit vector normal to $\Gamma_c'$. The non-penetration condition requires that $g$ is non-negative. At the same time the

normal contact traction $t$ can only be compressive or zero. Both conditions are usually written in the form of the Signorini condition

$$g \geq 0, \quad t \leq 0, \quad gt = 0. \tag{8}$$

The contact problem can now be formulated as a constrained minimisation problem [8, 11]. The functional to be minimised is the potential energy $\Pi(\mathbf{u})$ defined for all kinematically admissible displacements $\mathbf{u}$ (i.e. those satisfying $\mathbf{u} = \bar{\mathbf{u}}$ on $\Gamma_u^0$),

$$\Pi(\mathbf{u}) = \int_{\Omega^0} W(\mathbf{u}) \, dV - \int_{\Gamma_t^0} \bar{\mathbf{t}} \cdot \mathbf{u} \, dS, \tag{9}$$

where $W(\mathbf{u})$ is a strain energy function. The inequality constraint imposed on the displacement field $\mathbf{u}$ reflects the impenetrability condition, so that the deformation of the body $\mathbf{u}$ is found as a solution of the following minimisation problem

$$\min_{\mathbf{u}} \Pi(\mathbf{u})$$
$$\text{subject to } g(\mathbf{u}) \geq 0 \text{ on } \Gamma_c. \tag{10}$$

Alternatively, problem (10) can be written in a discretized form resulting from a finite element approximation. Denoting the global nodal displacement vector by $\mathbf{U}$, the minimisation problem (10) becomes

$$\min_{\mathbf{U}} \Pi(\mathbf{U})$$
$$\text{subject to } g_i(\mathbf{U}) \geq 0, \quad i = 1, \ldots, N_c, \tag{11}$$

where $N_c$ is the number of contact integration points and $g_i$ is a gap at the $i$-th contact integration point.

## 3.2 Penalty method

Among many solution methods available for constrained minimisation problems of type (10) the penalty method seams to be the most popular one in the practical finite element implementations of contact problems. This is mostly because its implementation is quite straightforward and it results in a pure displacement formulation. This is, however, at the expense of serious (and well known) disadvantages: the impenetrability condition is satisfied in an approximate manner and convergence problems are often encountered.

In the penalty approach the inequality constraint is regularized by modifying the potential energy functional according to

$$\Pi_p(\mathbf{u}) = \Pi(\mathbf{u}) + \int_{\Gamma_c^0} \frac{1}{2} \epsilon <g(\mathbf{u})>_-^2 \, dS, \tag{12}$$

or in a discretized setting

$$\Pi_p(\mathbf{U}) = \Pi(\mathbf{U}) + \sum_{i=1}^{N_c} \frac{1}{2} A_i \epsilon < g_i(\mathbf{U}) >_-^2, \tag{13}$$

where $<x> = \frac{1}{2}(x + |x|)$, $<x>_- = <-x>$ and $\epsilon > 0$ is a penalty parameter. In Eq. (13), $A_i$ is an equivalent area (in the reference configuration) associated with the $i$-th contact integration point, cf. [12].

The penalty regularization (13) transforms the constrained minimisation problem (11) into an unconstrained one, namely

$$\min_{\mathbf{U}} \Pi_p(\mathbf{U}). \tag{14}$$

The solution of problem (14) is found from the necessary condition of stationary point of $\Pi_p(\mathbf{U})$, namely

$$\nabla_{\mathbf{U}} \Pi_p(\mathbf{U}) = \mathbf{0}, \tag{15}$$

where $\nabla_{\mathbf{U}} = \partial/\partial\mathbf{U}$. Condition (15) constitutes the set of nonlinear equations for the global displacement vector $\mathbf{U}$, which can be written in a residual form $\mathbf{R}(\mathbf{U}) = \mathbf{0}$ corresponding to Eq. (1). Thus the formulation of direct and sensitivity analysis of Section 2 can directly be applied for the problem at hand. We note that the frictionless contact problem for an elastic body is actually not path-dependent, cf. the case of *steady-state nonlinear systems* in [6].

The scheme of the penalty method for frictional contact problems follows in essence that outlined above. Again a pure displacement formulation is obtained, however, the slip rule, being the part of the friction law, makes the problem path-dependent. Practical applications of the sensitivity analysis for two-dimensional frictional contact problems in penalty formulation can be found in [1, 2].

### 3.3 Augmented Lagrangian method

The augmented Lagrangian treatment of the contact and friction conditions is getting increased interest as the method allows for exact fulfillment of the inequality constraints and, even more importantly, provides more stable numerical schemes as compared to the penalty approach. In this section the approach developed in [7, 8] is briefly presented. As it is demonstrated below, this approach is particularly suitable for the sensitivity analysis.

For the case of frictionless contact an augmented Lagrangian functional is constructed

$$\mathcal{L}(\mathbf{u}, \lambda) = \Pi(\mathbf{u}) + \int_{\Gamma_c^0} \frac{1}{2\epsilon} \left( <\lambda + \epsilon g(\mathbf{u}) >_-^2 - \lambda^2 \right) dS, \tag{16}$$

where $\lambda$ is a dual field of Lagrange multipliers defined on the contact surface $\Gamma_c^0$ and $\epsilon > 0$ is a regularization parameter. A discrete counterpart of (16) reads

$$\mathcal{L}(\mathbf{U}, \boldsymbol{\Lambda}) = \Pi(\mathbf{U}) + \sum_{i=1}^{N_c} \frac{1}{2\epsilon} A_i \left[ <\lambda_i(\boldsymbol{\Lambda}) + \epsilon g_i(\mathbf{U}) >_-^2 - \lambda_i(\boldsymbol{\Lambda})^2 \right], \tag{17}$$

where $\lambda_i(\mathbf{\Lambda})$ results from the approximation of the Lagrange multiplier field $\lambda$ over the potential contact surface $\Gamma_c^0$ and is expressed in terms of the nodal vector of Lagrange multipliers $\mathbf{\Lambda}$. An important property of $\mathcal{L}(\mathbf{u}, \lambda)$ and $\mathcal{L}(\mathbf{U}, \mathbf{\Lambda})$ is that they are smooth and differentiable [8].

The contact problem can now be formulated as the following (unconstrained) saddle-point problem for the primal and dual variables $\mathbf{U}$ and $\mathbf{\Lambda}$

$$\min_{\mathbf{U}} \max_{\mathbf{\Lambda}} \mathcal{L}(\mathbf{U}, \mathbf{\Lambda}) \tag{18}$$

and the corresponding necessary conditions of the saddle point have the form

$$\begin{aligned} \nabla_{\mathbf{U}} \mathcal{L}(\mathbf{U}, \mathbf{\Lambda}) &= \mathbf{0}, \\ \nabla_{\mathbf{\Lambda}} \mathcal{L}(\mathbf{U}, \mathbf{\Lambda}) &= \mathbf{0}. \end{aligned} \tag{19}$$

Equations (19) can now be written in a residual form

$$\left\{ \begin{array}{c} \mathbf{R}_{\mathbf{U}}(\mathbf{U}, \mathbf{\Lambda}) \\ \mathbf{R}_{\mathbf{\Lambda}}(\mathbf{U}, \mathbf{\Lambda}) \end{array} \right\} = \left\{ \begin{array}{c} \mathbf{0} \\ \mathbf{0} \end{array} \right\}, \tag{20}$$

where $\mathbf{R}_{\mathbf{U}}$ and $\mathbf{R}_{\mathbf{\Lambda}}$ denote the parts of the global residual vector that originate from $\nabla_{\mathbf{U}}\mathcal{L}$ and $\nabla_{\mathbf{\Lambda}}\mathcal{L}$, respectively. The iterative Newton scheme (2) for the solution of the primal problem is rewritten here in the form corresponding to Eq. (20), namely

$$\left[ \begin{array}{cc} \mathbf{K}_{\mathbf{UU}} & \mathbf{K}_{\mathbf{U\Lambda}} \\ \mathbf{K}_{\mathbf{\Lambda U}} & \mathbf{K}_{\mathbf{\Lambda\Lambda}} \end{array} \right] \left\{ \begin{array}{c} \delta\mathbf{U} \\ \delta\mathbf{\Lambda} \end{array} \right\} = - \left\{ \begin{array}{c} \mathbf{R}_{\mathbf{U}} \\ \mathbf{R}_{\mathbf{\Lambda}} \end{array} \right\}, \qquad \left\{ \begin{array}{c} \mathbf{U} \\ \mathbf{\Lambda} \end{array} \right\}^{k+1} = \left\{ \begin{array}{c} \mathbf{U} \\ \mathbf{\Lambda} \end{array} \right\}^{k} + \left\{ \begin{array}{c} \delta\mathbf{U} \\ \delta\mathbf{\Lambda} \end{array} \right\}, \tag{21}$$

where $\mathbf{K}$ is a global tangent matrix and $\mathbf{K}_{\alpha\beta}$ denote its parts resulting from the division of the global vector of unknowns into nodal displacements $\mathbf{U}$ and Lagrange multipliers $\mathbf{\Lambda}$.

As shown above, the augmented Lagrangian treatment [7, 8] of contact fully fits into the general solution scheme of the primal problem of Section 2. Thus the sensitivity analysis framework of Section 2 can directly be applied. Naturally, frictionless contact results in a path-independent problem and, again, extending to the case of frictional contact does not change the picture significantly except that the problem becomes path-dependent.

We note that $\mathbf{K}$ in Eq. $(21)_1$ is the exact tangent operator of the problem so that sensitivity analysis is a single linear problem to be solved after the direct problem is solved (for a path-dependent problem of frictional contact this is done at each time step). This, however, is not the case of the Uzawa algorithm being another, in fact more popular, approach to augmented Lagragian method. That approach (see for example [3, 10, 11, 13]) involves two nested iteration loops. The inner loop is the Newton solution of the nonlinear problem (equilibrium) in primal variables (displacements), the dual variables (Lagrange multipliers) being fixed. This is followed by an update of the Lagrange multipliers. These two steps are repeated in an outer loop until convergence is obtained. Consequently, the exact sensitivity problem is also iterative and is computationally more expensive.

The interative solution of the sensitivity problem is avoided in [3] by adopting the penalty formulation with oversized penalties for the sensitivity problem, while the direct problem employs the augmented Lagrangian method and the Uzawa algorithm. This, however, leads to a deteriorated accuracy of the sensitivity analysis as opposed to the excellent agreement with the finite difference schemes that is usually obtained in the case of exact sensitivity analysis.

## 4 FINITE ELEMENT IMPLEMENTATION

The present finite element implementation is restricted to two-dimensional problems involving frictional contact with a rigid obstacle, the classical Coulomb law being used to model frictional interaction. The extension of the framework of Section 3.3 to frictional contact and the details of the contact formulation (e.g. definition of kinematic and static contact variables) are omitted here as they can be found in [8]. The augmented Lagrangian treatment of contact and friction conditions also follows that developed in [8].

Contact discretization is based on the one used to derive the extended node-to-segment element [12], except that contact with a smooth and rigid surface is only considered here. The contact element formed by a typical contact node $S$ involves two neighbouring nodes $N_1$ and $N_2$, Fig. 2, which allow for consistent treatment of the equivalent area $A_i$ of the element (see [12] for the discussion on surface-expansion-dependent contact laws and [2] for sensitivity analysis-related topics). Two Lagrange multipliers, representing the normal and the tangential contact tractions, constitute additional degrees of freedom of the element.
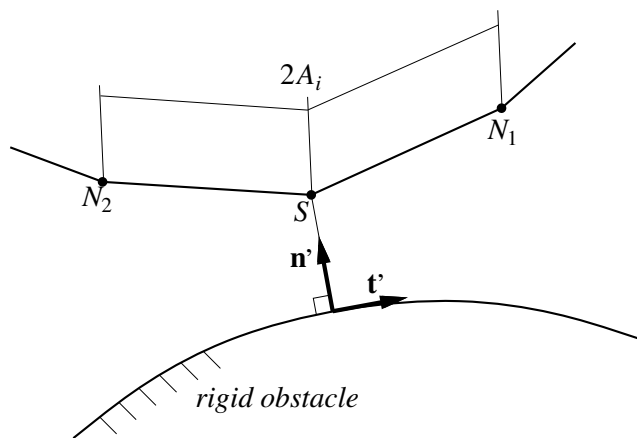


Figure 2: Extended contact element.

The finite element implementation and the computations were performed within the *Computational Templates* environment [14] and a symbolic code generation system *Ace-Gen* [15, 16], extending the symbolic capabilities of *Mathematica* [17], was used to derive and automatically generate the numerical code.

## 5 EXAMPLES

### 5.1 Plane strain frictionless Hertz problem

A plane strain problem of frictionless contact of a rigid cylinder with an elastic half-space is studied. The half-space is approximated by a rectangular block and a prescribed indentation force $P$ is applied as an uniform pressure at the bottom of the block, Fig. 3. The parameters of the problem are: Young's modulus $E = 100\,\text{N/mm}^2$, Poisson's ratio $\nu = 0.3$, indentation force $P = 1.2\,\text{N/mm}$, cylinder radius $R = 1\,\text{mm}$.
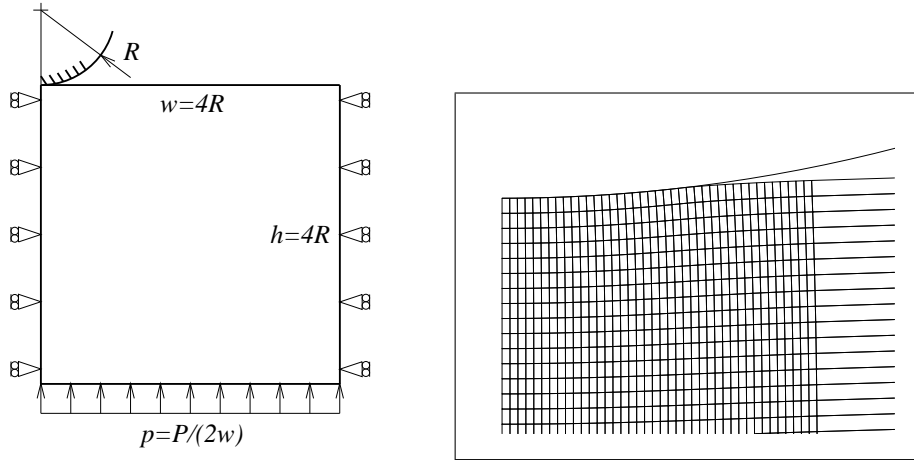


Figure 3: Plane strain Hertz problem: geometry and the detail of deformed mesh.

The well known analytical solution of the plain strain Hertz contact problem [18] provides the following distribution of contact pressure $p_N$

$$p_N(x) = p_N^0 \sqrt{1 - \left(\frac{x}{a}\right)^2}, \quad a = \sqrt{\frac{4PR(1 - \nu^2)}{\pi E}}, \quad p_N^0 = \frac{2P}{\pi a}. \tag{22}$$

The sensitivity of the contact pressure with respect to the variation of cylinder radius can easily be obtained by differentiating relations (22). The distributions of contact pressure $p_N$ and its sensitivity $\mathrm{D}p_N/\mathrm{D}R$ (at constant indentation force $P$) computed using the DDM-based finite element scheme are shown in Fig. 4. As it is seen, a very good agreement with the respective analytical distributions is obtained.

### 5.2 Plane strain frictional Hertz problem

This example extends the previous one by considering friction (the geometry and parameters of the problem are those of Section 5.1, except that the cylinder radius is $R = 10\,\text{mm}$, the maximum force is $P = 1.5\,\text{N/mm}$ and friction coefficient $\mu = 0.3$ is assumed). As discussed in Section 3.3, friction makes the problem path-dependent.
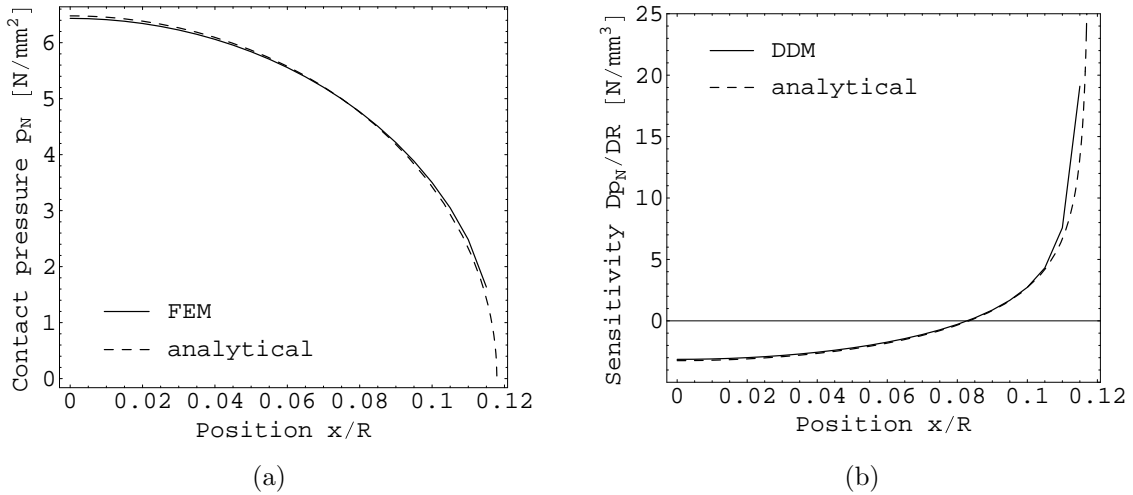
Figure 4: Plane strain Hertz problem: distribution of (a) contact pressure and (b) its sensitivity with respect to cylinder radius variation.

The problem is self-similar so that, as the load increases, the contact, sticking and frictional sliding zones evolve in a self-similar manner. Thus this simple problem can be used for assessing the accuracy of the method (of both direct and sensitivity analysis) by checking its ability to represent evolving contact states. The normal and friction tractions corresponding to $P_1 = 0.5\,\text{N/mm}$, $P_2 = 2P_1$ and $P_3 = 3P_1$ are shown in Fig. 5. In order to check how the self-similarity is captured by the finite element model, the normalized distributions of contact pressures are provided in Fig. 6(a,b). The contact pressures are normalized by dividing by the theoretical maximum pressure $p_{Ni}^0$ corresponding to the current force $P_i$, cf. Eq. $(22)_3$, and the position $x$ is normalized using the theoretical current contact radius $a_i$, cf. Eq. $(22)_2$.
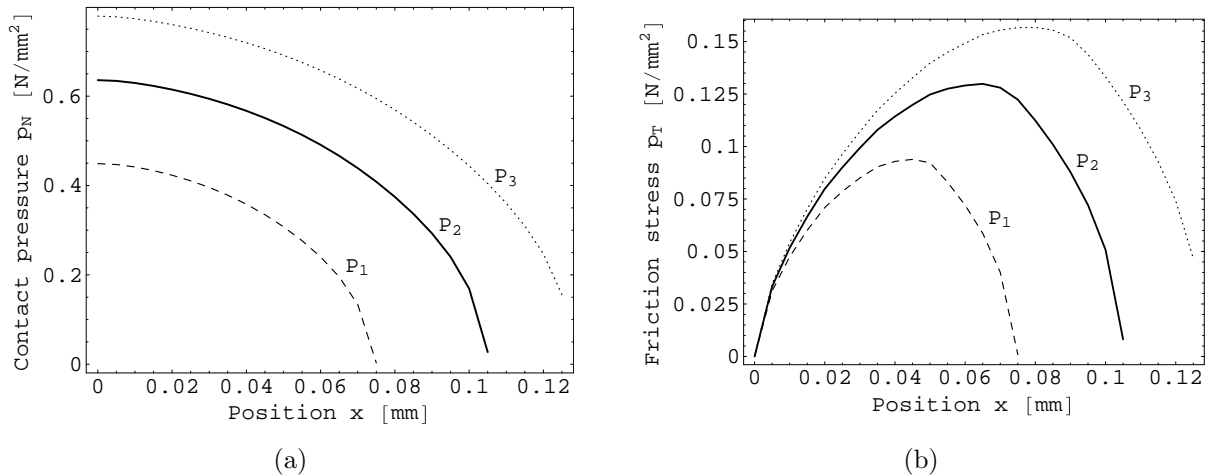


Figure 5: Frictional Hertz problem: distribution of (a) contact pressure and (b) friction stress.

(a)

(b)

(c)

(d)
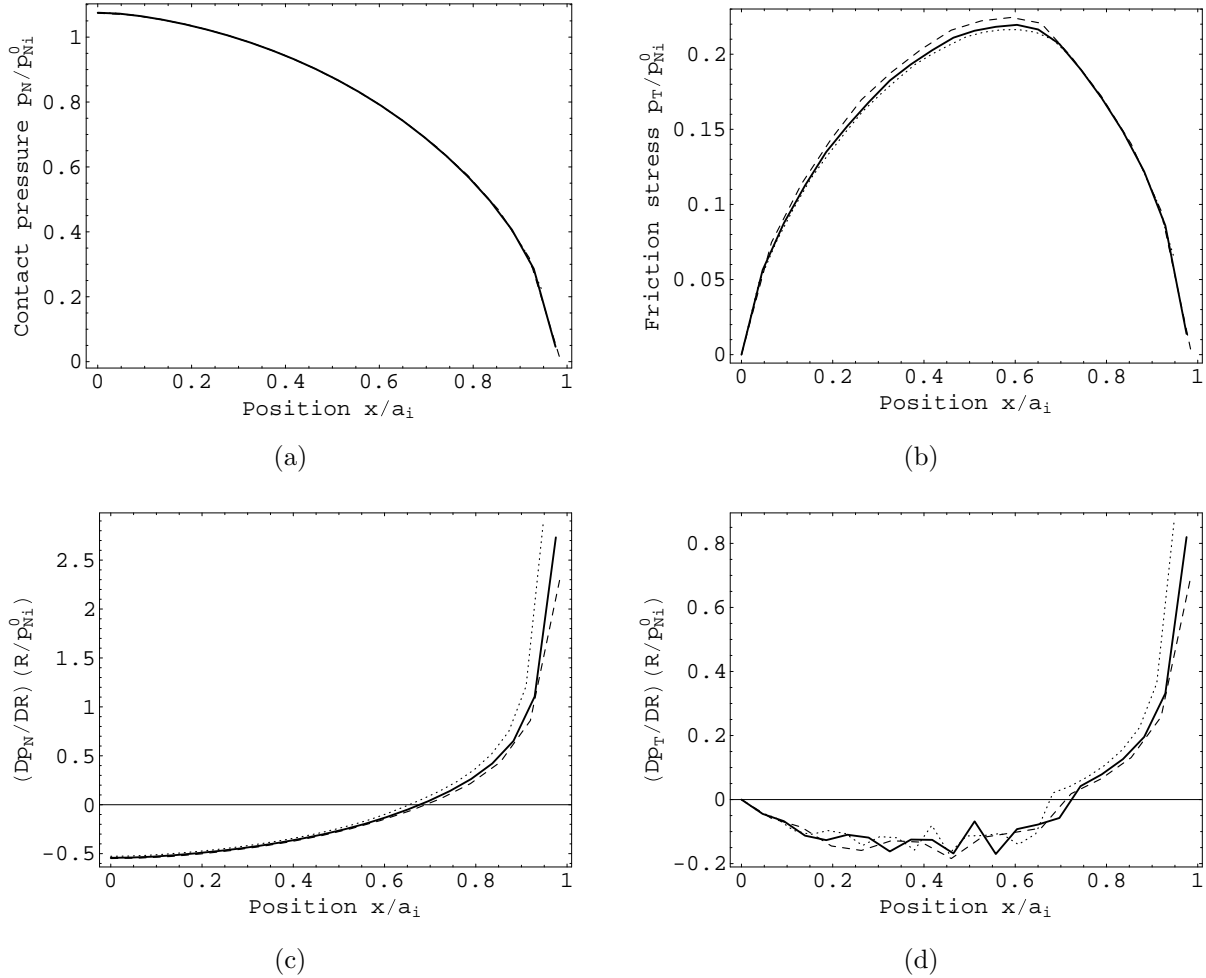
Figure 6: Frictional Hertz problem: normalized distributions of contact pressures and of their sensitivity with respect to the variation of cylinder radius.

Normalized sensitivities of contact pressures with respect to the variation of cylinder radius are shown in Fig. 6(c,d). The sensitivities are divided by $p_{Ni}^0$ and additionally multiplied by the radius $R$, so that the normalized sensitivity of normal pressure is given by $(\mathrm{D}p_N/\mathrm{D}R)(R/p_{Ni}^0)$. From Fig. 6 it follows that the self-similar nature of the solution is reproduced properly, although some discretization error is visible, particularly in the case of sensitivities.

## 5.3   Optimisation of free boundary shape in forging

This example is an application of sensitivity analysis for an academic, metal forming-oriented shape optimisation problem. Consider a cylindrical billet which is compressed between two flat, rigid dies. As depicted in Fig. 7 the billet bulges due to the frictional interaction with the die. Now, the problem is to find the initial shape of the billet such

11

that after upsetting the billet is cylindrical [19, 3].
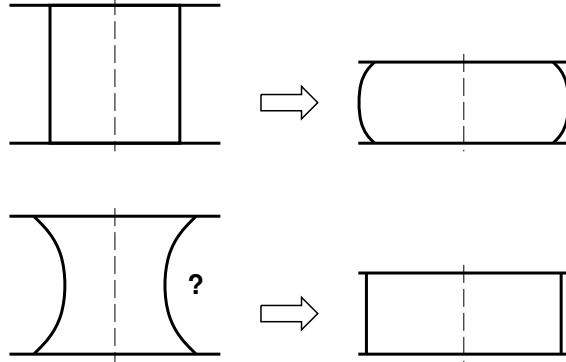


Figure 7: Optimisation of free boundary shape in forging.

The problem is axisymmetric and due to symmetry only one half of the cross-section is modelled. The initial shape of the billet is defined using Bézier polynomials with the Bernstein basis functions, namely

$$r_0(\xi) = \sum_{i=0}^{m} \phi_i f_i(\xi), \quad f_i(\xi) = \binom{m}{i} \xi^i (1 - \xi)^{m-i}, \quad \xi = \frac{z}{h_0}, \tag{23}$$

where $r_0(\xi) = r_0(y/h_0)$ denotes the radius of the billet as a function of the distance $z$ from the symmetry plane, $2h_0$ is the initial height of the billet and $\phi_i$ are shape parameters. Bézier polynomials of degree four are used ($m = 4$), so that five shape parameters describe the initial shape of the billet.

The material model of the billet is an elasto-plastic model based on finite deformation $J_2$-flow theory [20]. A four-noded, isoparametric, displacement-based element with selective reduced integration is used ($E = 10^4\,\mathrm{MPa}$, $\nu = 0.3$, $\sigma_y = 100\,\mathrm{MPa}$). Coulomb friction is assumed on the tool-workpiece contact interface.

The objective function corresponding to the optimisation problem stated above can be written as

$$F(\boldsymbol{\phi}) = \sum_k [r_k(\boldsymbol{\phi}) - r_{\mathrm{opt}}]^2, \tag{24}$$

where $r_{\mathrm{opt}}$ is the desired radius of the billet and $r_k$ denotes the final position (in the radial direction) of node $k$ on the free surface. Naturally, the latter depends on the vector of shape parameters $\boldsymbol{\phi}$ both explicitly, through the initial shape of the billet, and implicitly, through the nodal displacement. In this example, 50 per cent height reduction is applied and the desired radius is $r_{\mathrm{opt}} = h_0$.

The accuracy of the DDM-based sensitivity analysis has been verified against the sensitivities obtained using the finite difference scheme (FDM). The results obtained for an initially cylindrical billet, $\phi_0 = \ldots = \phi_4 = 0.7h_0$, are provided in Table 1. As it is

12

| Shape | $\mathrm{D}F/\mathrm{D}\phi_i$ | | Relative |
| parameter | DDM | FDM | difference |
| --- | --- | --- | --- |
| $\phi_0$ | 0.05930 | 0.05924 | -0.100% |
| $\phi_1$ | -0.08022 | -0.07998 | -0.304% |
| $\phi_2$ | -0.29431 | -0.29467 | 0.123% |
| $\phi_3$ | -0.57618 | -0.57594 | -0.043% |
| $\phi_4$ | -2.45970 | -2.45975 | 0.002% |

Table 1: Comparison of DDM and FDM sensitivities (FDM step $\Delta\phi_i/h_0 = 10^{-6}$).

seen a very good agreement with the FDM scheme is obtained for the FDM perturbation $\Delta\phi_i/h_0 = 10^{-6}$.

Optimal initial shapes of the billet are shown in Fig. 8 for different values of the friction coefficient $\mu$. The effect of friction on the optimal shape is clearly visible in Fig. 8. As could be expected higher friction coefficients require larger variation of the initial radius. The convergence history of the BFGS algorithm [21] used in this study is illustrated in Fig. 9.



(a) $\mu = 0.1$  (b) $\mu = 0.2$  (c) $\mu = 0.3$
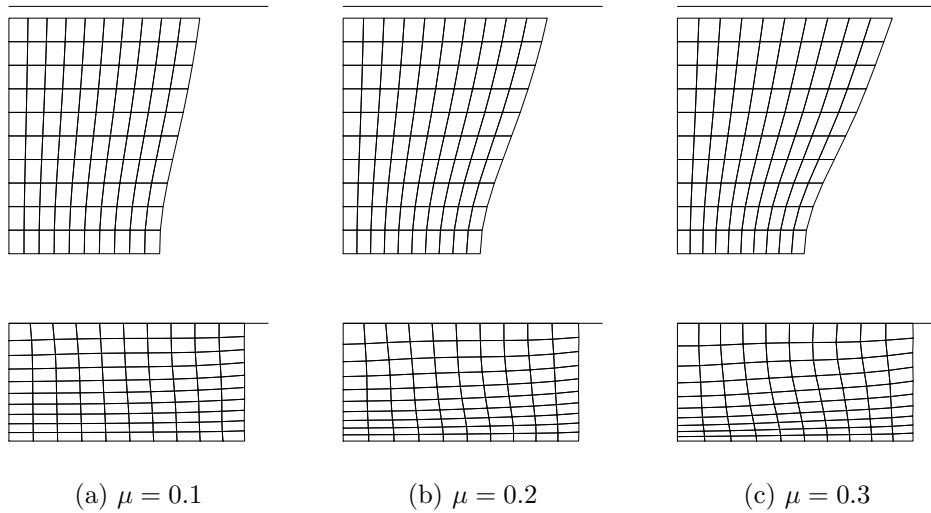
Figure 8: Optimisation of free boundary shape in forging: undeformed (optimised) and deformed mesh.

## 6  CONCLUSION

Sensitivity analysis is developed for frictional contact problems in augmented Lagrangian formulation. The augmented Lagrangian treatment of friction and contact conditions proposed in [7, 8] and used in this study appears to be particularly suitable for the sensitivity analysis. This is because the direct problem is solved using a Newton-type scheme for the primal (displacements) and dual (Lagrange multipliers) variables simulta-
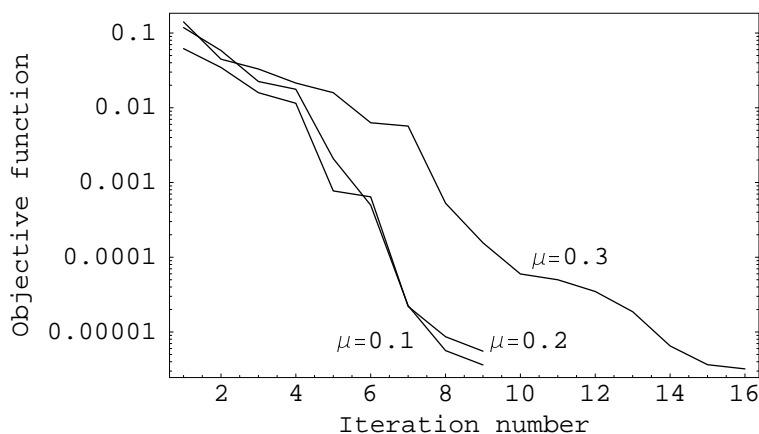
Figure 9: Optimisation of free boundary shape in forging: convergence of the optimisation algorithm.

neously and the tangent operator of the Newton scheme is the exact tangent operator of the problem. Thus the sensitivity problem is only a single linear problem at each time increment (this is not the case of the augmented Lagrangian method combined with the Uzawa algorithm).

Numerical examples illustrate the accuracy of the DDM-based sensitivity analysis and its applicability for optimisation problems. Note that the sensitivity analysis can also be used to investigate the properties of numerical schemes and accuracy of obtained solutions. The augmented Lagrangian method is expected to provide solutions which do not depend on the regularization parameter $\epsilon$. Indeed, it has been verified that taking $\epsilon$ as a 'design' parameter provides response sensitivities equal to a numerical zero.

# REFERENCES

[1] N.H. Kim, K.K. Choi, J.S. Chen, and Y.H. Park. Meshless shape design sensitivity analysis and optimization for contact problem with friction. *Comp. Mech.*, 25(2–3):157–168, 2000.

[2] S. Stupkiewicz, J. Korelc, M. Dutko, and T. Rodič. Shape sensitivity analysis of large deformation frictional contact problems. *Int. J. Num. Meth. Engng.*, 191(33):3555–3581, 2002.

[3] A. Srikanth and N. Zabaras. Shape optimization and preform design in metal forming processes. *Comp. Meth. Appl. Mech. Engng.*, 190:1859–1901, 2000.

[4] J.J. Tsay and J.S. Arora. Nonlinear structural design sensitivity analysis for path dependent problems. Part I: General theory. *Comp. Meth. Appl. Mech. Engng.*, 81:183–208, 1990.

[5] M. Kleiber. Shape and non-shape structural sensitivity analysis for problems with any material and kinematic non-linearity. *Comp. Meth. Appl. Mech. Engng.*, 108:73–97, 1993.

[6] P. Michaleris, D.A. Tortorelli, and C.A. Vidal. Tangent operators and design sensitivity formulations for transient non-linear coupled problems with applications to elastoplasticity. *Int. J. Num. Meth. Engng.*, 37:2471–2499, 1994.

[7] P. Alart and A. Curnier. A mixed formulation for frictional contact problems prone to Newton like solution methods. *Comp. Meth. Appl. Mech. Engng.*, 92:353–375, 1991.

[8] G. Pietrzak and A. Curnier. Large deformation frictional contact mechanics: continuum formulation and augmented Lagrangian treatment. *Comp. Meth. Appl. Mech. Engng.*, 177(3–4):351–381, 1999.

[9] M. Kleiber, H. Antunez, T.D. Hien, and P. Kowalczyk. *Parameter Sensitivity in Nonlinear Mechanics*. Wiley, Chichester, 1997.

[10] T.A. Laursen. *Computational Contact and Impact Mechanics*. Springer-Verlag, Berlin, 2002.

[11] P. Wriggers. *Computational Contact Mechanics*. Wiley, Chichester, 2002.

[12] S. Stupkiewicz. Extension of the node-to-segment contact element for surface-expansion-dependent contact laws. *Int. J. Num. Meth. Engng.*, 50:739–759, 2001.

[13] T.A. Laursen and J.C. Simo. A continuum-based finite element formulation for the implicit solution of multibody, large deformation frictional contact problems. *Int. J. Num. Meth. Engng.*, 36(20):3451–3485, 1993.

[14] J. Korelc. Computational Templates. Available at http://www.fgg.uni-lj.si/Symech/, 2000.

[15] J. Korelc. Automatic generation of finite-element code by simultaneous optimization of expressions. *Theor. Comp. Sci.*, 187:231–248, 1997.

[16] J. Korelc. Automatic generation of numerical codes with introduction to AceGen 4.0 symbolic code generator. Available at http://www.fgg.uni-lj.si/Symech/, 2000.

[17] S. Wolfram. *The Mathematica Book, 4th ed.* Wolfram Media/Cambridge University Press, 1999.

[18] K.L. Johnson. *Contact Mechanics.* Cambridge University Press, 1985.

[19] L. Fourment, T. Balan, and J.L. Chenot. Optimal design for non-steady-state metal forming processes — II. Application of shape optimization in forging. *Int. J. Num. Meth. Engng.*, 39:51–65, 1996.

[20] J.C. Simo and F. Armero. Geometrically nonlinear enhanced mixed methods and the method of incompatible modes. *Int. J. Num. Meth. Engng.*, 33:1413–1449, 1992.

[21] W.H. Press, S.A. Teukolsky, W.T. Vetterling, and B.P. Flannery. *Numerical Recipes in Fortran 77: The Art of Scientific Computing.* Cambridge University Press, 1992.